Edge Estimation and Restoration of Gaussian Degraded Images

Ziya Telatar*† and Önder Tüzünalp‡

Ankara University Faculty of Science, Department of Electronic Engineering, 06100-Besevler, Ankara, Turkey

The blur function of a degraded image is often unknown a priority. The blur function must first be estimated from the degraded image data before restoring the image. We propose an algorithm to address the blur estimation problem. The present algorithm based on the estimation of restoration filter parameters by using edge information of the degraded image is presented to solve the restoration problem of the degraded image. The information that relates the variance of the Gaussian blur kernel on degraded image is considered. Simulation results of image restoration illustrate the performance of the proposed estimation method.

Journal of Imaging Science and Technology 42: 370–374 (1998)

Introduction

The restoration of images degraded by blur is still a central problem in image processing. Blur can be introduced by atmospheric turbulance, improperly focused lenses, relative motion, or other environmental factors between an object being photographed and an image scanner. The restoration of degraded images differs in each case.

The problem of deblurring of images with known blur function has been dealt with extensively in the literature. The restoration algorithms include Fourier domain methods (inverse filtering,[1–3] blind deconvolution,[3–5] Cepstrum,[6–8] etc.) or spatial domain methods.[9] In many applications, however, the blur function is unknown. Therefore, the estimation or identification of blur function directly from the blurred image has been a focus of great deal of interest. A number of techniques have been proposed to address this problem.

Chang, Tekalp, and Erdem[10] have proposed a blur identification algorithm in which an observed image has been segmented into N segments by using a method for blur identification. Reeves and Mersereau[11] have used a generalized cross validation method for blur identification. Kayargadde and Martens[12] have used polynomial transformations to estimate the edge parameters and image blur.

Although several methods exist to restore degraded images, there is still room for improvement.[3] In this work we propose a new algorithm for restoration of unknown Gaussian blurred images using edge estimation. The proposed algorithm follows an iterative scheme to converge the blur function and then restores the degraded image after a certain number of iterations. The following sections present the blur model, our restoration algorithm, experimental results, and conclusions.

Problem Identification and the Proposed Method

In this work, we address the problem of deconvolution of unknown Gaussian degradation from an edge estimation. To describe our techniques, we begin in this section with a brief description of a blurred image, and state some important properties relating to it.

Generally, a blurred image can be modeled as follows:

$$y(n_1,n_2) = \mathrm{g}(n_1,n_2)*h(n_1,n_2) + v(n_1,n_2), \tag{1}$$

where the original image $g(n_1,n_2)$ has been blurred by the function $h(n_1,n_2)$ with an additive noise $v(n_1,n_2)$. Additive noise may come from the imaging system independent of the original image. Additive noise degradation model parameters of imaging systems are known. Thus, additive noise may be easily removed from the degraded image by using special image processing techniques such as Wiener filtering before the restoration. Therefore the additive noise problem has been left out here; rather, we refer the reader to Refs. 1 through 5 and 9 for further details.

Neglecting the additive noise, Eq. 1 can be rewritten as,

$$y(n_1,n_2) = g(n_1,n_2)*h(n_1,n_2). \tag{2}$$

Equation 2 states that degradation is the result of the convolution between the original scenery and the blur function.

The blur function $h(n_1,n_2)$ given in Eq. 2 could have statistically different distributions, and different models could be identified for each distribution problem. As a result, the restoration problem may become very complex. In so far as the Gaussian distribution includes all other distributions, in general, we assume that all blurring effects have Gaussian, or normal, distribution. For example, atmospheric turbulence, unfocused imaging systems, motion, or evaporation effects could cause the

Original manuscript received October 3, 1997

* IS&T Member

† e-mail: telatar@eros.science.ankara.edu.tr ; TEL: ++90 312 2126720/1145; FAX: ++90 312 223 23 95

‡ e-mail: tuzunalp@eros.science.ankara.edu.tr ; TEL: ++90 312 2126720/1221; FAX: ++90 312 223 23 95

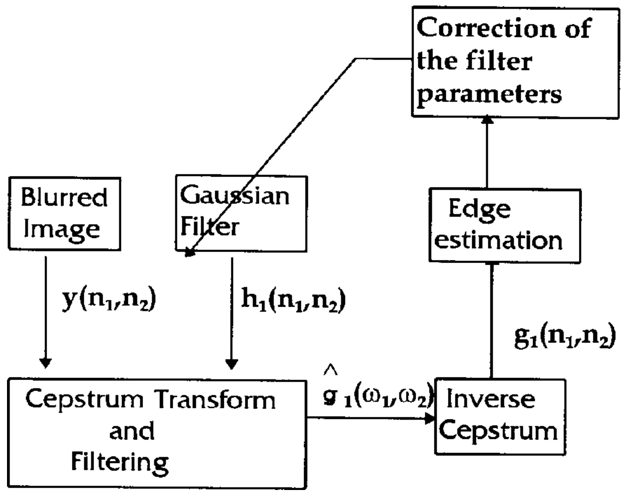

Figure 1. Edge estimation and restoration algorithm block diagram.

original image to blur with Gaussian distribution. A Gaussian distribution can be modeled as,

$$h_1(n_1,n_2) = \frac{1}{2\pi\sigma^2} e^{-\frac{(n_1^2+n_2^2)}{2\sigma^2}}. \tag{3}$$

Equation 3 represents the filter model in which the variance and the matrix size have an effect on the filter performance. This model will be used for the restoration of the blurred image. As long as the variance and the matrix size can be appropriately arranged, a good approximation of the original image should be obtained.

In this study, we use the gradient edge detection method[3] to estimate the filter model parameters. In a blurred image, regions of high frequency, called edge pixels are spread over the neighboring pixels causing the loss of image details. Thus, the blurred image edge map does not contain more edge lines or points than the original one. Using this property, we can say that the edge map of an image contains important information about the degradation.

Figure 1 shows a block diagram for the algorithm. The process to converge to the blur function of the degraded image is as follows:

Step 1. Find the edge map of the actual image.
Step 2. Choose the filter model parameters, variance and matrix size from step 1.
Step 3. Construct a filter using the parameters in step 2.
Step 4. Restore the degraded image.
Step 5. Find the edge map of step 4.
Step 6. Compare step 5 and previous edge map. If step 5 > the previous edge map, filter parameters are actual, else filter parameters are the previous.
Step 7. Choose the next value of the filter parameters.
Step 8. Construct a new filter and repeat steps 5 through 8.

After a certain number of iterations, the best edge map gives the best filter model parameters used for designing the restoration filter. (Note that different variances are used for a fixed matrix size of filter model in the algorithm. In other words, the variance is searched for a fix blur matrix size, then the matrix size is changed.) There for each iteration step:

$$b^{i+1} = b^i + \Delta b^i[n_1(i+1); n_2(i+1)], \tag{4}$$

where, b^{i+1} is the convergency vector of the model coefficients and Δb^i is the correction term that depends on the measurements along a period.

The choice of the amplitude level of the edge points is particularly important because the edge algorithm may detect low noise as an edge point. To obstruct the false edges, first, we introduced a fixed threshold (k). Then, we chose the amplitudes up to the fixed threshold as an edge point. Here if k is low, noise may be detected as an edge point. If k is high, some edge points may not be detected. Thus, the threshold level k has been chosen as 35% of the amplitude of the maximum edge pixel level. As a result, the relation between the variance and the edge algorithm is defined as,

$$\sigma^2 = f(\nabla) = \left\{\sum\sum\left[\nabla y(n_1;n_2) \geq k\right]\right\}_{\max}. \tag{5}$$

where σ^2 is the variance, ∇ is the gradient operator, and y is the blurred image. Equation 5 is used to compute appropriate matrix size and variance for the restoration filter model.

Having estimated the filter model parameters, we use the Fourier domain Cepstrum transform for the filtering. The Cepstrum algorithm has been extensively used for image processing applications and its features are well documented in the literature.[3,6–8] Fourier domain Cepstrum transform of Eq. 2 is obtained as,

$$y'(\omega_1,\omega_2) = g'(\omega_1,\omega_2) + h'(\omega_1,\omega_2). \tag{6}$$

Equation 6 shows that the blur function is decomposed into a sum of original scenery of the image component and blur effect component by using the Fourier domain Cepstrum transformation.

Let the designed filter be $h_1(n_1,n_2)$ after the iterations and the filtering process in Cepstrum domain as,

$$y'(\omega_1,\omega_2) = g'(\omega_1,\omega_2) + h'(\omega_1,\omega_2) - h'_1(\omega_1,\omega_2) \tag{7}$$

Minimizing of the error between the blur function model parameters and the constructed filter model parameters presents the improvement of the quality in the image.

Mean squared prediction error is then computed to obtain the restoration error:

$$E = \sum_{n_1}\sum_{n_2}\left[g(n_1,n_2) - y_{new}(n_1,n_2)\right]^2, \tag{8}$$

where $g(n_1,n_2)$ and $y_{\text{new}}(n_1,n_2)$ are the original and restored images, respectively. The energy of the original signal E_1 is defined by

$$E_1 = \sum_{n_1}\sum_{n_2}\left[g(n_1,n_2)\right]^2. \tag{9}$$

To evaluate the improvement in the restored image, we combine Eqs. 8 and 9,

$$I = 20\log_{10}\frac{E_1}{E}. \tag{10}$$

Experimental Results

The performance of the proposed algorithm has been investigated with three different types of blurred images. The restoration results are presented in this section with a 200×200 pixel simulated child image, a real world degraded

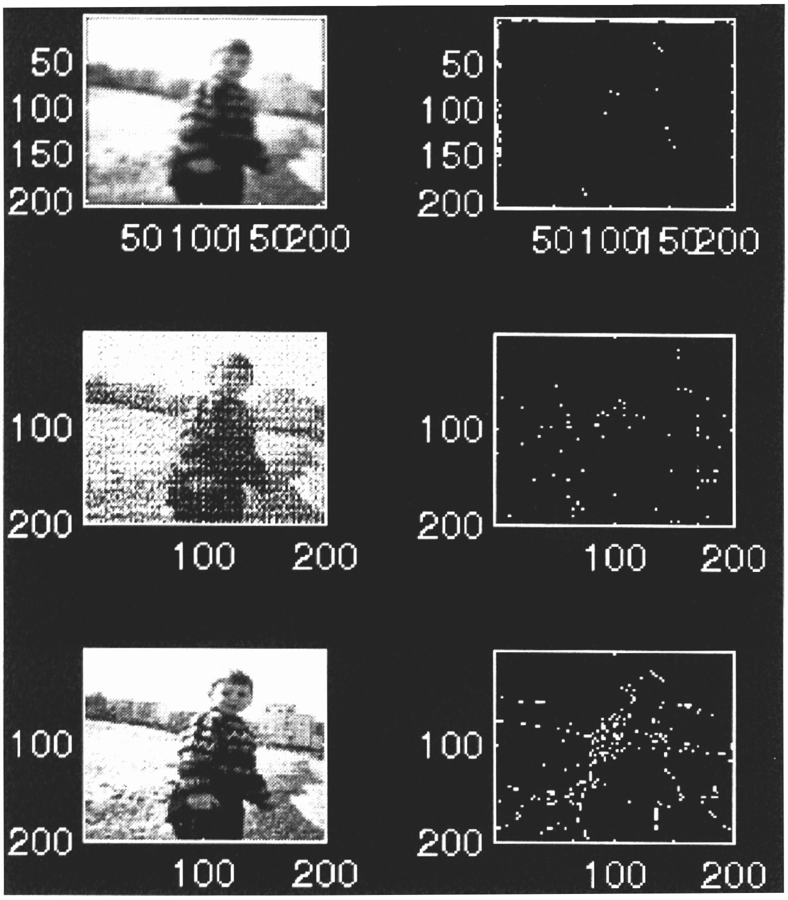

Figure 2. (a) Blurred child image with variance 13.75 (left above); (b) edge map of (a) (right above); (c) restored image by filter not estimated correctly from degraded image (middle left); (d) edge map of (b) (middle right); (e) resulting image from (e), (left below); (f) edge map of result of iterations (right below).

TABLE I. Mean Square Error Measurement in Blurred and Restored Child Image

Image	Estimated Variance	MSE in blurred image	MSE in restored image	Improvement (dB)
	5.5 (7 × 7 pix.)	1145.3	4.811	75.8
Child	10.25 (13 × 13 pix.)	2400.0	4.988	75.5
(Fig.-2.)	13.75 (13 × 13 pix.)	3154.1	6.463	73.3

TABLE II. Restoration Results in the Real World Images

Images	Estimated Variance	Improvement	Image type
Fig. 3	5	26.6	Photographic
Fig. 4	3	28.7	Satellite
Fig. 5	7	26.4	Satellite
Fig. 6	4	30.15	Satellite

photographic image, and a real world satellite image. The proposed algorithm estimates the size and variance of blur function from the blurred image and restores it.

Figures 2(a) and 2(b) show the Gaussian blurred child image and its edge map in which image details have been lost. It is seen that not enough edge pixels are on the edge map. Figures 2(c) and 2(d) show restoration results from an incorrectly estimated filter parameter. So, the image is still not very clear. Figures 2(e) and 2(f) present the restored image and its edge map. The threshold operation prevents the edge pixels from detection of small noise as an edge point. The performace of the restoration is shown by the improvement in the image quality in Table I.

The algorithm has also been applied to real life degraded images and considerable improvement has been observed in the resulting images. Figures 3(a) and 3(b) show an original photograph image and its edge map. The image was blurred by out of focus lenses. Degradation again has a Gaussian distribution. The restoration result of the image is depicted in Fig. 3(c) and its edge map in Fig. 3(d). Table II also presents the improvement in image quality.

Figures 4(a), 5(a), and 6(a) show some real world satellite images taken by the Hubble Space Telescope. These images have been degraded by atmospheric turbulence. Thus, some details on the images have been lost. The restored images are shown in Figs. 4(c), 5(c), and 6(c) respectively. Improvements in all of the satellite images are considerable as given in Table II.

Conclusion

This paper develops a new restoration algorithm for unknown Gaussian degraded images. Variance and matrix size of the convolutional Gaussian effect are estimated and accordingly the blurred image is restored. Our experimental results show that the proposed method performs effective restoration for degraded images. If the original scene has only been degraded by the blur function as in the case of the simulated child image, the restoration result is satisfactory. However, there are some unmeasured observation effects in real world images and these effects cannot be controlled. Our filter model partially compensates unmeasured observation effects but not all. So the restoration results and improvements for the real world images given in Table II are not as high performance as in the simulated image.

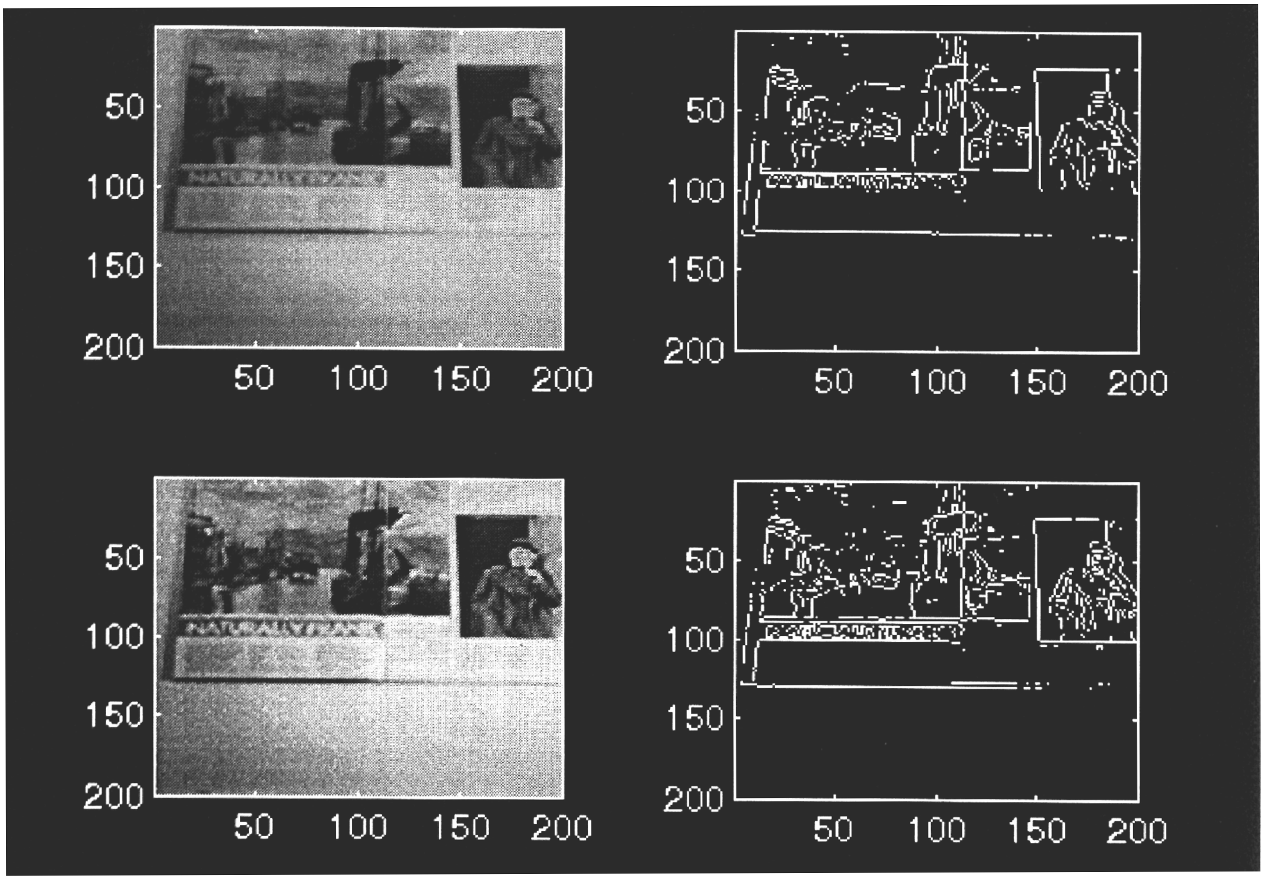

Figure 3. (a) A real world photograph image (left above); (b) edge map of (a) (right above); (c) restored image from (a) (left below; (d) edge map of (c).

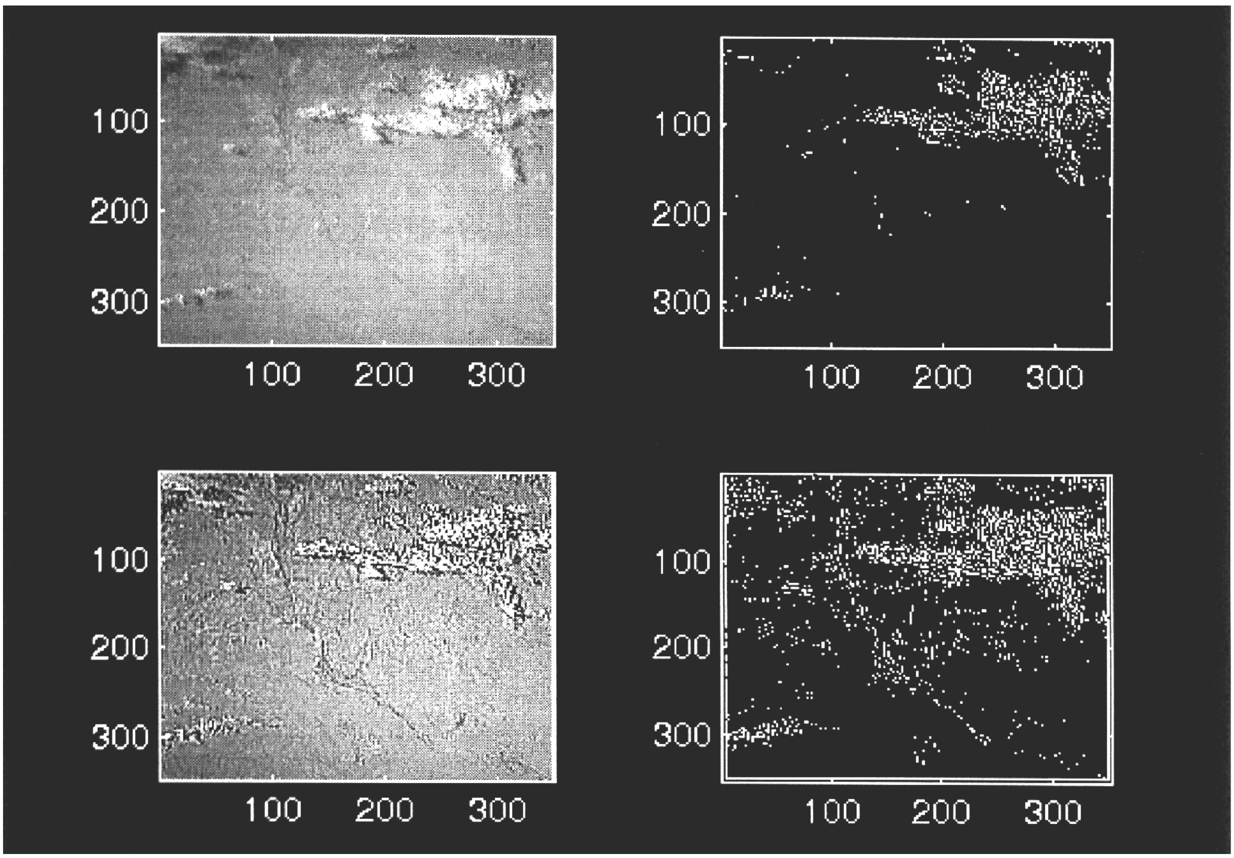

Figure 4. (a) A real world satellite image (left above); (b) edge map of (a) (right above); (c) restored image from (a) (left below; (d) edge map of (c).

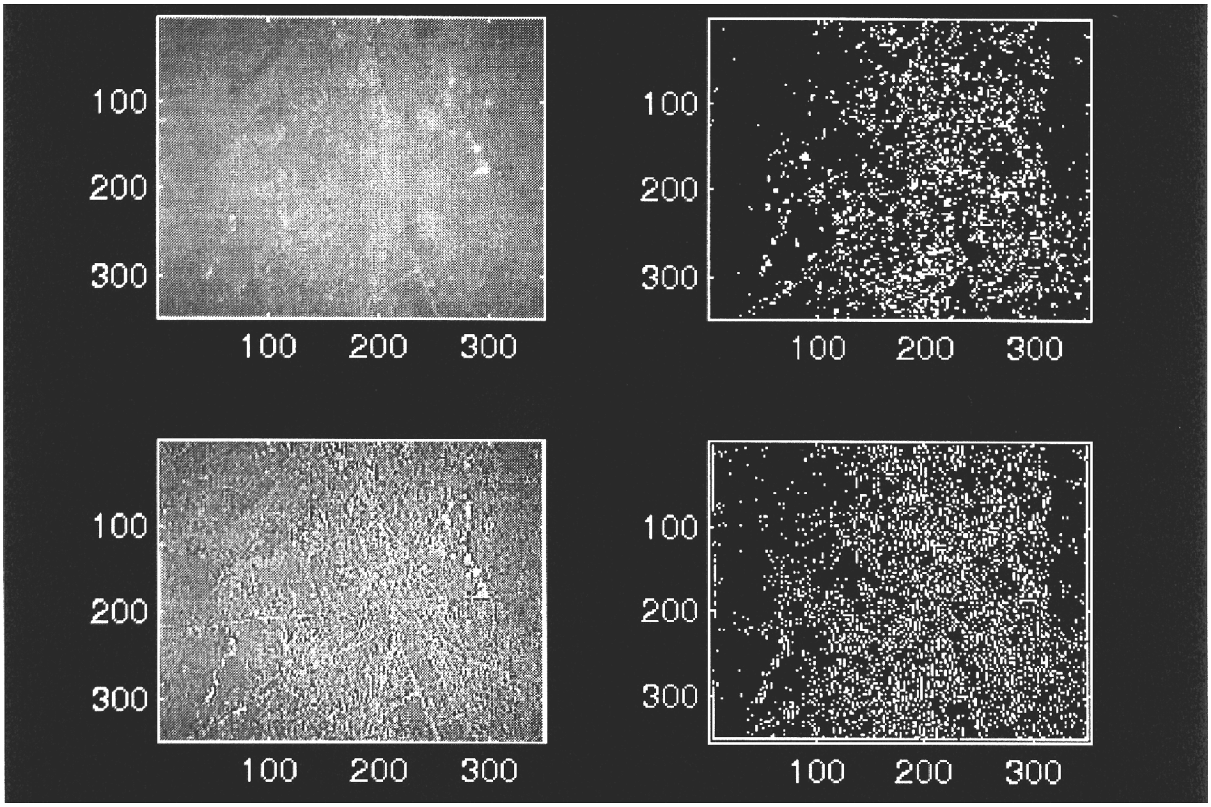

Figure 5. (a) A real world satellite image (left above); (b) edge map of (a) (right above); (c) restored image from (a) (left below; (d) edge map of (c).

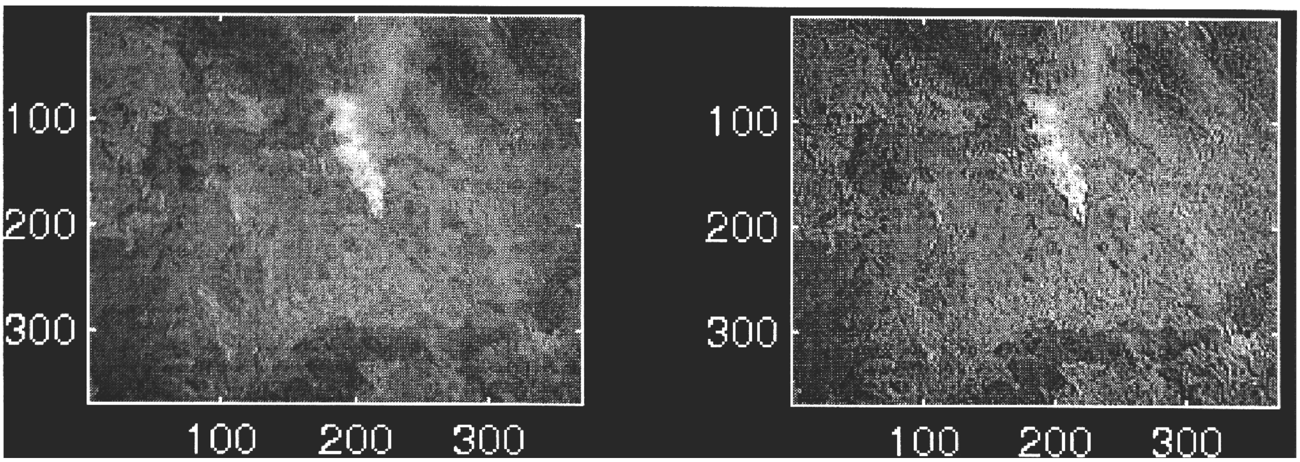

Figure 6. (a) A real world satellite image (left); (b) restored image from (a) (right).

The algorithm needs 125 iteration steps with 43 min required on a 90-MHz Pentium computer. If the matrix size is chosen properly, iteration steps can be reduced to 20 with very low computing time, which can be important for real-time applications. Under these conditions, restoration quality may decrease, however.

References

1. B. L. McGlamery, Restoration of turbulence-degraded images, *J. Opt. Soc. Amer.* **57**, 293 (1967).
2. G. M. Robbins and T. S. Huang, Inverse filtering for linear shift variant imaging systems, *Proc. IEEE* **60,** 862 (1972).
3. J. S. Lim, *Two Dimensional Signal and Image Processing*, Prentice Hall,1990.
4. J. W. Goodman, *Introduction to Fourier Optics*, McGraw Hill, 1968.
5. S. C. Pohlig, New techniques for blind deconvolution, *Opt. Eng.* **20**, 281 (1981).
6. D. E. Dudgeon, The computation of two dimensional Cepstra, *IEEE Trans. Acoust. Speech Signal Proc.* **ASSP-25,** 476 (1977).
7. J. K. Lee, M. Kabrisky, M. E. Oxley, S. K. Rogers, and D. W. Ruck, The complex Cepstrum applied to two-dimensional images, *Patt. Recog.* **26**, 1579 (1993).
8. P. A. Petropulu and C. L. Nikias, The complex Cepstrum and Bicepstrum: Analytic performance evaluation in the presence of Gaussian noise, *IEEE Tran. Acoust. Speech Signal Proc.* **38,** 1246 (1990).
9. O. Shunichiro, Restoration of images degraded by motion blur using matrix operators, *Int. J. Systems Sci.* **22,** 937 (1991).
10. M. M. Chang, A. M. Tekalp and A. T. Erdem, Blur identification using bispectrum, *IEEE Trans. Signal Proc.* **39,** 2323 (1991).
11. S. J. Reeves and R. M. Mersereau, Blur identification by the method of generalized cross-validation, *IEEE Trans. Image Proc.* **1,** 301 (1992).
12. V. Kayargadde and J. B. Martens, Estimation of edge parameters and image blur using polynomial transforms, *CVGIP* **56**, 442 (1994).
13. G. Demoment, Image reconstruction and restoration: Overview of common estimation structures and problems, *IEEE Trans. Acoust. Speech Signal Process.* **37,** 2024 (1989).
14. Z. Telatar, Adaptive restoration of blurred satellite images, in ISI 51st Session of the International Statistical Institute, Book 2**,** 499, (1997).
15. Y. Ando, A. Hansuebsai and K. Khantong, Digital restoration of faded color images by subjective method, *J. Imag. Sci. Tech.* **41,** 259 (1997).